Strong Gravitational Lensing in the Era of Big Data
Proceedings IAU Symposium No. 381, 2024
H. Stacey, A. Sonnenfeld & C. Grillo, eds.
doi:10.1017/S1743921323004052

Combined strong and weak gravitational lensing mass measurements in clusters of galaxies

Davide Abriola

University of Milan. email: davide.abriola@unimi.it

Abstract. Gravitational lensing in clusters of galaxies is one of the most powerful methods to probe the dark matter mass distribution inside such systems, after mapping the baryonic component, and test the currently accepted ΛCDM cosmological paradigm. With the advent of new high-resolution facilities such as the JWST, strong lensing (SL) is capable of providing extremely accurate mass measurements in the densest regions of such structures. Weak lensing (WL) provides complementary information by measuring the total mass distribution in the outskirts of galaxy clusters, where no multiple images of background sources are produced.

In my talk, I will present updates on the WL mass reconstruction of the Frontier Fields galaxy cluster Abell 2744 ($z = 0.308$) based on Subaru, Magellan, and JWST data, and I will show how the results obtained, combined with accurate SL modeling of this lens, provide a consistent picture of the cluster total mass distribution. I will discuss the pipeline used for this work, the extensive checks performed on the different datasets and the scientific results obtained. Being composed of several substructures undergoing a merging process, the complex geometry of this cluster makes it an ideal laboratory to verify the consistency and reliability of the results obtained with the two methods. I will compare the predictions of the SL models extrapolated in the outer regions of the cluster with the non-parametric WL mass reconstruction to look for potential systematic effects affecting the SL analysis.

Keywords. Cosmology: observations – dark matter – Galaxies: clusters: individual (Abell 2744) – Gravitational lensing: weak

1. Introduction

Galaxy clusters have been proved to be powerful cosmological probes: indeed, being among the most massive systems of the Universe, they constitute the most recent phase of the hierarchical structure formation, and thus represent the ideal laboratory to study the evolution and interaction between galaxies. For several applications, it is crucial to rigorously map their total mass distribution: e.g., once the baryonic component has been mapped, one can infer the physical properties of dark matter and hence shed new light on its nature. These findings can then be compared with the results of cosmological simulations, in order to test the currently accepted ΛCDM structure formation paradigm. Gravitational lensing is, for this purpose, one of the most robust tools we have at our disposal, since, differently from other methods, it does not rely on stringent hypotheses about the physical nature, state or composition of the deflecting mass. Thanks to the extremely high density of their inner cores (up to hundreds of kpc from their centres), galaxy clusters can act as strong gravitational lenses, capable of producing elongated arcs and hundreds of multiple images of background sources that otherwise could not be observed.

If one wants to map the total mass distribution up to the less dense outskirts of a cluster (i.e., up to few Mpc from their cores), where no multiple images are formed, then weak lensing (WL) provides a complementary and independent probe. The statistical study of the slight distortion induced on the shape of background galaxies allows indeed for a robust and model-free reconstruction of the total mass distribution. Hence, combined strong and weak lensing studies allow one to map the projected total mass of the deflectors on different scales, and an excellent agreement between the two probes has been reported in several clusters.

Among the most massive clusters, Abell 2744 (lying at redshift $z = 0.308$) shows one of the most complex merger phenomena ever observed, detected both in the radio and in the X-ray. A recent WL analysis (Medezinski et al. 2016) based on Subaru/Suprime-Cam imaging yielded new evidence to support this picture, by discovering the presence of four substructures undergoing multiple mergers. More recently, thanks to its peculiarity, this system has been the target of still ongoing surveys, including the Beyond Ultra-deep Frontier Fields And Legacy Observations (BUFFALO) survey, as well as the James Webb Space Telescope (JWST) Early Release Science (ERS) program Grism Lens Amplified Survey from Space (GLASS).

In this talk, I will present a new WL analysis of the galaxy cluster Abell 2744 using deep Magellan/MegaCam multi-band imaging data covering a field of view of approximately $31' \times 33'$. The analysis has been carried out with brand-new shape measurement and PSF reconstruction softwares, which we first tested on less deep Subaru/Suprime-Cam data of the same system. We will show the various tests performed to look for possible sources of systematics, in order to obtain a robust WL mass distribution which does not suffer from the dilution due to foreground sources. Finally, we will compare our result with the afore-mentioned WL analysis and a complementary strong lensing (SL) study.

2. A brief recall of WL methodology

We carried out our WL reconstruction starting from the measurements of the shapes of background galaxies, i.e., lying at a higher redshift than the lens (for a review see, e.g., Bartelmann & Schneider 2001). Given these measurements, we first recover the two-dimensional *shear* field γ induced by the gravitational potential of the deflector through a moving average over a pixelized grid. We then reconstruct the total surface mass density distribution Σ of the cluster from γ by applying the procedure first introduced by Lombardi & Bertin (1998): indeed, it can be shown that the gradient of Σ can be expressed as a suitable combination of the derivatives of γ. Therefore we can minimize the difference between the measured γ and such gradient to recover the expected surface mass density.

3. Data description

We performed the WL analysis of the galaxy cluster Abell 2744 by applying a brand-new pipeline for the measurement of the spatial variation of the point spread function (PSF) and the shapes of background galaxies. For this reason, we first tested the analysis softwares on Subaru/Suprime-Cam BR_cz' imaging data of the same cluster, covering a field of view of approximately $24' \times 27'$. After this preliminary study, we analyzed new data collected in 2018 with the MegaCam camera, located at the $f/5$ focus of the 6.5-m Magellan 2 Clay telescope at Las Campanas Observatory, Chile. The observations were carried out in the three filters g, r, and i, and from them an effective $\simeq 31' \times 33'$ composite image was processed. The observation details of both the instruments are listed in Table 1.

https://doi.org/10.1017/S1743921323004052 Published online by Cambridge University Press

Table 1. The specifics of the observations.

Instrument	Filter	Exp. time [10^4 s]	$m_{\rm lim}$ (AB mag)	FWHM [$''$]
MegaCam	g	2.04	28.7	0.541
	r	1.20	28.4	0.487
	i	4.80	27.8	0.520
Suprime-Cam	B	0.21	27.9	1.16
	R_c	0.31	27.7	1.23
	z'	0.36	27.5	0.91

Notes: $m_{\rm lim}$ denotes the 5σ limiting magnitude within a Kron-like aperture. The point spread function (PSF) standard deviation was estimated as the median of the detected star FWHM size distribution. The latter measurements were realized in order to produce a color-composite image of the cluster, on which we performed the analysis.

We first identified the astronomical sources located on the field of view with the software SExtractor (Bertin & Arnouts 1996), and we later classified them either as galaxies or stars by studying their distribution in size and magnitude. Following this method, we identified 695 objects as stars and 86945 as galaxies.

Afterwards, we further distinguished the galaxies between potential cluster members and background ones. To do so, we relied on the procedure outlined by Medezinski et al. (2010, 2018). We studied the distribution of the galaxies in a color-color (CC) space and, for each CC cell, evaluated the mean distance from the cluster centre†. We thus restricted to the region occupied by those galaxies having the smallest distance from the centre (less than 6 Mpc), and assumed them to likely be cluster members. Since the contamination between cluster members and background galaxies represents one of the primary sources of systematic uncertainties in WL, we verified *a posteriori* the purity and completeness of our cluster galaxies sample by comparing it to the deep VLT/MUSE spectroscopic redshift catalog presented by Bergamini et al. (2023a), containing the redshifts of thousands of galaxies located within few arcmins from the BCG. Through this comparison, we achieved an accuracy of $\simeq 93\%$ and a precision of $\simeq 83\%$. Finally, we isolated the foreground galaxies from the background ones by relying once again on the CC-space methodology described above: we thus obtained a catalog consisting of 54614 potentially background galaxies, corresponding to an average number density of $\simeq 54\,{\rm galaxies/arcmin}^{-2}$.

4. Analysis

4.1. *Shape measurement*

The measurement of the shapes of background galaxies represents one of the most crucial steps in WL analysis, since they have to be measured with high accuracy. It is therefore necessary to carefully take into account the effects induced by the PSF, since it introduces an artificial shape distortion, and properly correct for them. This can be done by measuring the shapes of the stars located on the field of view: stars are indeed ideally point-like sources. Therefore, if they appear extended and/or distorted, this is likely due to the PSF: hence, measuring the shapes of observed stars allows one to quantify its effects. We reconstructed the spatial variation of the PSF all over the field of view with the software mccd (Liaudat et al. 2021).

We then proceeded with the measurements of the shapes of the background galaxies with the module ngmix (Sheldon 2015; Sheldon & Huff 2017). At the end of this step,

† assumed to be the south-east brightest cluster galaxy (BCG).

https://doi.org/10.1017/S1743921323004052 Published online by Cambridge University Press

we had to clean our sample by removing galaxies with an high error on the shape measurement, galaxies with a overlapping isophotes, etc. This left us with 13942 background galaxies to compute the mass distribution with, i.e., $\simeq 15$ galaxies/arcmin^2.

We thus reconstructed the shear field γ. To do so, we pixelized the field of view onto a $480\,\mathrm{px} \times 500\,\mathrm{px}$ grid and introduced an isotropic two-dimensional Gaussian weight function with standard deviation equal to $0.5'$. Since background galaxies are distributed in redshift, it was necessary to weigh them according to their distance in a proper manner. To do so, we estimated their redshift distribution by comparing our sample with the photometric redshift catalog centered in the Hubble Deep Field - North (HDF-N) by Yang et al. (2014), after dividing the galaxies per magnitude bin.

4.2. *Mass reconstruction*

Finally, we reconstructed the total surface mass distribution Σ by implementing the method outlined by Lombardi & Bertin (1998). We estimated a statistical error σ_k on this reconstruction through a *reshuffling* procedure (Lombardi & Bertin 1999), i.e., we produced further 120 mass density maps, each time shuffling the coordinates of the background galaxies, and evaluated the standard deviation on the resulting realizations of Σ.

Eventually, we looked for potential systematic effects. Firstly, we evaluated the so-called B-modes† and verified they were consistent with a null signal. Secondly, we took care of the *mass-sheet degeneracy* by estimating the value of the additional constant to add Σ to. We modelled the main density peak identified in our surface mass distribution (the one in the south-east part of the cluster, see later) in terms of a softened pseudo-isothermal elliptical mass distribution (SPIEMD), depending, among the other parameters, on the additive constant. We determined the parameters of the model by means of a Bayesian inference.

5. Results

At a distance of 2 Mpc from the south-east BCG, we recovered a total mass of $(2.5 \pm 0.2) \times 10^{15}\,\mathrm{M}_\odot$, thus making Abell 2744 one of the most massive clusters. To further corroborate the validity of our results, we compared our findings with the SL study by Bergamini et al. (2023b) based on new deep, high-resolution JWST imaging, after extrapolating their best-fit model up to 700 kpc. As can be seen in the *right* panel of Figure 1, where both the best-fit SL model and the WL surface mass distributions are overlaid on a Magellan g-band extract of the field of view, a good agreement emerges. Only a slight discrepancy is present, likely due to the presence of a saturated star in the Magellan images at our disposal. As a further test, we compared the cumulative radial mass profiles emerging from both the probes, that are displayed in Figure 2. As can be seen, our findings are in a nice agreement within one σ_k.

Our analysis reveals the presence of three density peaks (having a S/N greater than 7), all of which lying in correspondence of those observed in the SL surface mass distribution from Bergamini et al. (2023b). A slight overlap with the locations of the substructures detected in the aforementioned WL study by Medezinski et al. (2016) (the *blue* crosses in the *left* panel of Figure 1) is also observed. In particular, the south-east sub-structure detected by the authors of the study lies well within our density peak, as well as the

† Indeed, the two components of the complex shear can be decomposed into two parts, the so-called $E-$ (curl−free) and the $B-$ (divergence−free) modes. In the context of WL, the latter is identically zero, therefore the presence of non-null $B-$signal can thus be used as a test for the presence of systematic effects (e.g., for a review see Umetsu 2020). To do so, we evaluated Σ after rotating each component of the shear of an angle $\pi/4$ and estimated the rms error on the distribution obtained this way by means of a similar reshuffling procedure.

https://doi.org/10.1017/S1743921323004052 Published online by Cambridge University Press

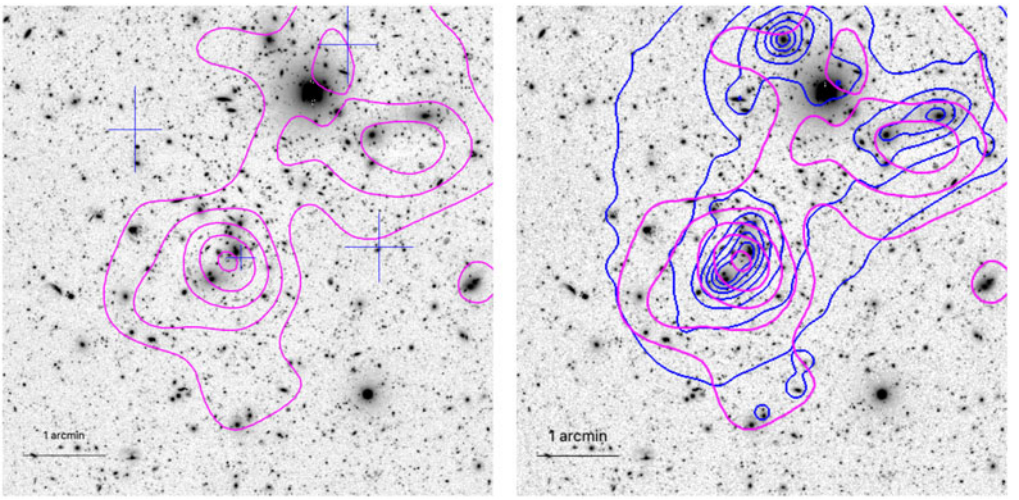

Figure 1. The central $6' \times 6'$ region of the Magellan/MegaCam g-band image with overlaid the contour levels of our surface mass distribution, in *magenta*. *Left*: the *blue* crosses denote the density peaks identified by Medezinski et al. (2016). *Right*: overlaid are also the contour levels of the surface mass distribution emerging from the SL study (Bergamini et al. 2023b, *blue*), referred to the same reference values.

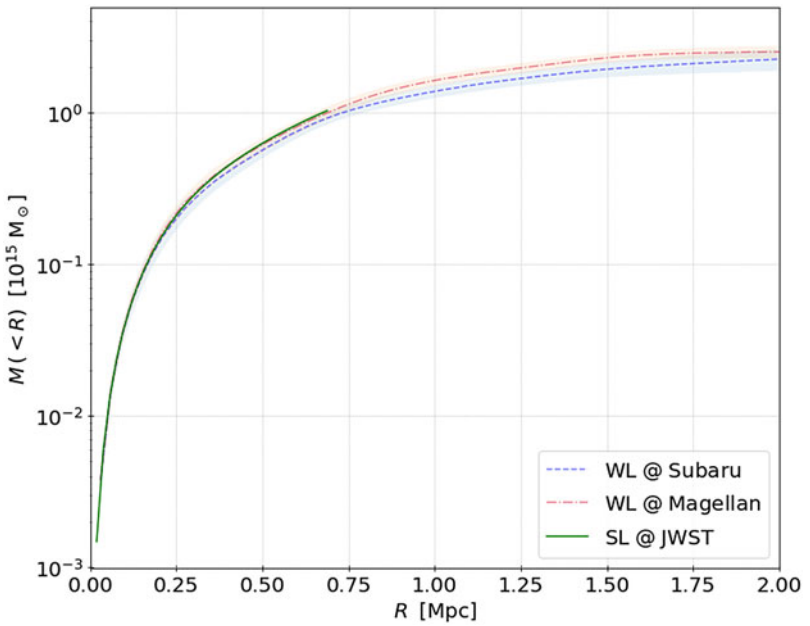

Figure 2. The cumulative radial total mass profile of the cluster in log-scale as obtained with Subaru/Suprime-Cam (blue), on which we first tested the pipeline described in the text, and Magellan/Megacam (red) imaging. Also shown is the cumulative profile (green) in the core of the cluster as a result of the SL analysis based on JWST (Bergamini et al. 2023b). The shaded area denotes the error band corresponding to one rms.

https://doi.org/10.1017/S1743921323004052 Published online by Cambridge University Press

north-west one. This result suggests that the cluster is not relaxed, but is undergoing a complex merging process, as supported by previous papers.

References

Bartelmann, M. & Schneider, P., 2001, Physics Reports, 340, 291
Bergamini, P., Acebron, A., Grillo, C. et al., 2023, A&A, 670, A60
Bergamini, P., Acebron, A., Grillo, C. et al., 2023, arXiv:2303.10210
Bertin, E. & Arnouts, S., 1996, A& ASuppl. Ser., 117, 393
Liaudat, T., Bonnin, J., Starck, J. L., et al., 2021, A&A, 646, A27
Lombardi, M. & Bertin, G., 1998, A&A, 330, 791
Lombardi, M. & Bertin, G., 1999, A&A, 348, 38
Medezinski, E., Broadhurst, T., Umetsu, K., et al., 2010, MNRAS, 405, 257
Medezinski, E., Umetsu, K., Okabe, N., et al., 2016, ApJ, 817, 24
Medezinski, E., Oguri, M., Nishizawa, A. J., et al., 2018, PASJ, 70, 30
Sheldon, E. & Huff, E. M., 2017, ApJ, 841, 24
Sheldon, E., 2015, Astrophysics Source Code Library, record ascl:1508.008
Umetsu, K., 2020, A&A Rev., 28, 7
Yang, G., Xue, Y. Q., Luo, B., et al., 2014, ApJS, 215, 27